UPDATE ON FEL PERFORMANCE FOR SWISSFEL

E. Prat and S. Reiche, PSI, Villigen, Switzerland

Abstract

The SwissFEL project under construction at the Paul Scherrer Institute foresees for 2017 the realization of an X-ray FEL with a photon wavelength down to 1 Å. In this paper we present the expected SASE performance for SwissFEL based on input distributions obtained from detailed start-to-end simulation results. The effects of the longitudinal wakefields due to resistive wall and surface roughness in the undulator beamline have been taken into account. We have studied and optimized the impact on the FEL performance of different factors like the electron focusing or the undulator tapering. Results for the standard cases with 200 pC and 10 pC electron bunch charge are shown.

INTRODUCTION

The SwissFEL facility, presently under construction at the Paul Scherrer Institute, will provide SASE and self-seeded FEL radiation at a hard (1-7 Å) and soft (7-70 Å) X-ray FEL beamlines [1]. SwissFEL will operate with electron beam charges varying between 10 and 200 pC and beam energies from 2.1 to 5.8 GeV. Two standard operational modes are foreseen: 1) the long-pulse (LP) mode to maximize the FEL output energy, with an electron beam charge of 200 pC and a rms bunch length of 18.4 fs; and 2) the short-pulse (SP) mode with 10 pC beam charge and 2.5 fs pulse duration.

In this document we present the SASE simulation results for the hard X-ray beamline and the two described operational modes. We have done the calculations for the shortest and longest radiation wavelengths, i.e. 1 Å and 7 Å. We have optimized the average β-function along the undulator beamline as well as the undulator tapering. We present the effects of the wakefields in the undulator beamline, showing that tapering can be employed to reduce the wakefields impact to a negligible level.

LAYOUT AND SIMULATIONS SETUP

The present design lattice for the hard X-ray beamline consists of 12 undulator modules. Each of them is 4 m long, has a period length of 15 mm and a variable gap with a nominal value of 4.2 mm. The distance between modules is 0.75 m. In addition we have reserved the space corresponding to an undulator module to place a magnetic chicane and a Bragg crystal to be used for self-seeding [2]. The facility is able to accommodate up to seven more modules for potential future upgrades such as long post-saturation tapering. A quadrupole magnet in the middle of each section between undulators is employed for beam focusing.

Figure 1 shows the properties of the electron beam distributions that we used as input for the FEL simulations for 1 Å. The distributions have been obtained by tracking with the simulation codes *ASTRA* [3] and *elegant* [4].

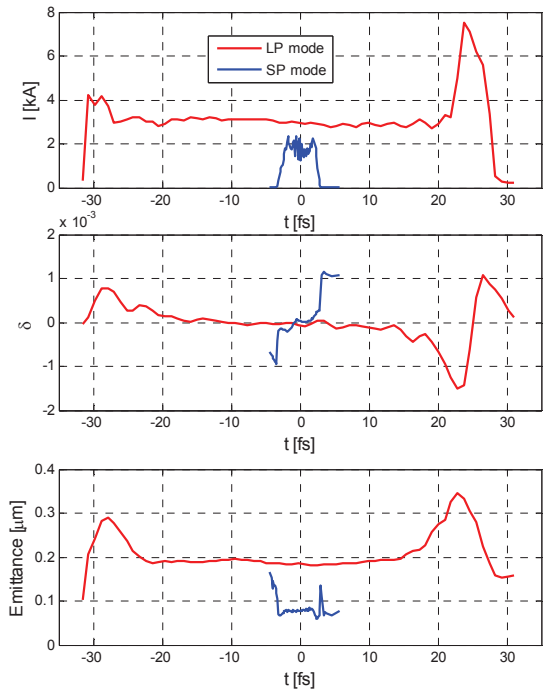

Figure 1: Electron beam slice properties at the undulator entrance for the LP mode (red) and SP mode (blue). Current profile (top), relative energy deviation (center) and normalized emittance (bottom).The emittance is defined as the geometrical average of the horizontal and vertical emittances.

The lasing at a radiation wavelength of 1 Å is obtained when the electron beam has a maximum energy of 5.8 GeV, which corresponds to an undulator parameter K of about 1.2. For the long wavelength (7 Å) we choose the undulator parameter as large as possible to maximize the beam energy and, as a consequence, to enhance the FEL output power. The maximum K is about 1.5, which corresponds to a beam energy of about 2.4 GeV. The particle distributions for 7 Å are obtained simply by scaling the distributions at 1 Å. This scaling is valid since the difference between the two configurations is only the energy provided by the last part of the linac, while keeping the same compression setup. The FEL interaction is simulated with *Genesis* [5].

FOCUSING OPTIMIZATION

We have analyzed how the FEL performance varies as a function of the focusing along the undulator for the LP mode. Figure 2 shows the relative FEL power at saturation as a function of the β-function for the two

ISBN 978-3-95450-133-5

radiation wavelengths. For 1 Å, the best SASE performance is obtained when the average β-function along the undulator is 10-11 m. For the 7 Å case the optimum β-function would be smaller or equal to 9 m, which is the minimum value that can be obtained in our lattice. For the SP mode we expect to have smaller optimum β-functions, since the emittances for this mode are also smaller. We have chosen for all succeeding simulations an average β-function along the undulator of 10 m, a compromise between the different optimums.

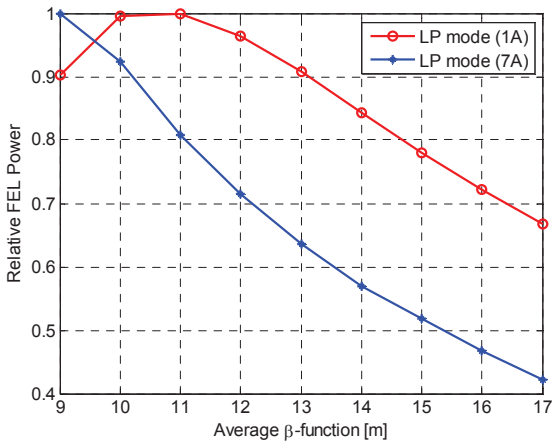

Figure 2: Relative FEL power at saturation as a function of the β-function along the undulator for the LP mode for a radiation wavelength of 1 Å and 7 Å.

FEL PERFORMANCE

Tapering the undulator helps to improve the FEL performance because it compensates the energy loss of the electrons due to lasing. For the two modes we have applied two stages of linear tapering: pre-saturation taper to optimize the gain length in the exponential regime and post-saturation taper to maximize the FEL power at the end of the undulator beamline. As an illustration example, Figure 3 shows the FEL macropulse energy at the end of the undulator as a function of the post-saturation taper amplitude for the LP mode at a radiation wavelength of 1 Å.

Table 1 shows the SASE properties at the undulator exit for the studied cases, namely the FEL macropulse energy, the FEL pulse duration (rms), the spectrum bandwidth (rms), the radiation divergence (rms) and the effective source point. These results correspond to only one shot noise seed. Due to the stochastic nature of the SASE process, the output energy fluctuates roughly proportionally to $n_s^{-1/2}$, being n_s the number of spikes of the SASE pulse. According to this, the FEL energy fluctuations are expected to be the following: about 38 % for the SP mode at 7 Å (7 spikes), about 17 % for the SP mode at 1 Å (35 spikes), and better than 10 % for the LP mode (more than 100 spikes).

Figures 4 and 5 show the FEL energy along the undulator beamline and the radiation spectrum, respectively, for the optimum case for all the considered configurations.

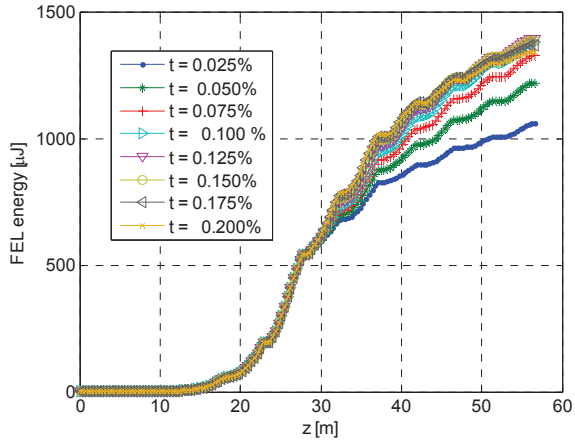

Figure 3: FEL macropulse energy for different post-saturation tapers. The maximum FEL energy is around 1.4 mJ and corresponds to a linear taper amplitude of 0.125% per undulator module.

Table 1: FEL Properties for the Different Studied Cases

	FEL Energy [μJ]	Rms length [fs]	Rms Spect. Band.	Rms div. [μrad]	Source point [m]
LP / 1 Å	1390	17.7	0.21%	2.0	20.4
LP / 7 Å	1650	17.0	0.45%	9.8	~10
SP / 1 Å	108	1.5	0.12%	1.6	24.2
SP / 7 Å	78	1.7	0.35%	8.5	~10

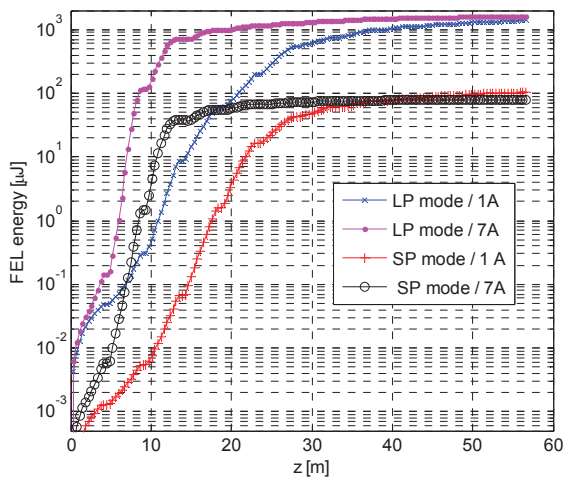

Figure 4: FEL macropulse energy along the undulator beamline for the different operational modes. The simulations are done per each case with the optimum focusing and undulator tapering.

ISBN 978-3-95450-133-5

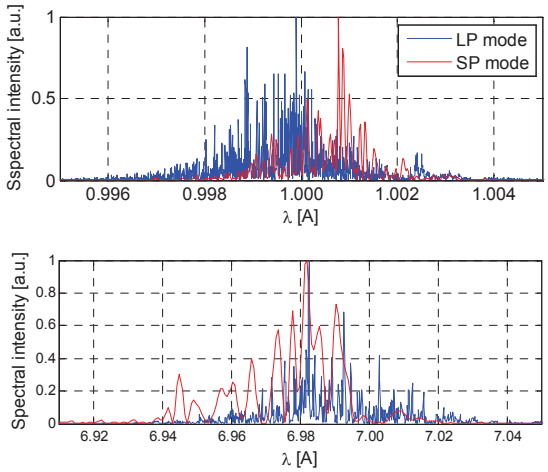

Figure 5: Radiation spectrum for the different operational modes for a wavelength of 1 Å (top) and 7 Å (bottom). The simulations are done with the optimum focusing and undulator tapering.

As an example, Figure 6 shows the divergence and the effective waist position along the undulator beamline for the LP mode at a radiation wavelength of 1 Å. The source position is calculated following the procedure described in Ref. [6]. For 7 Å we could not follow this procedure mostly due to slippage effects. For this case we have estimated the source point to be at about 2 gain lengths before saturation, i.e. at around 10 m.

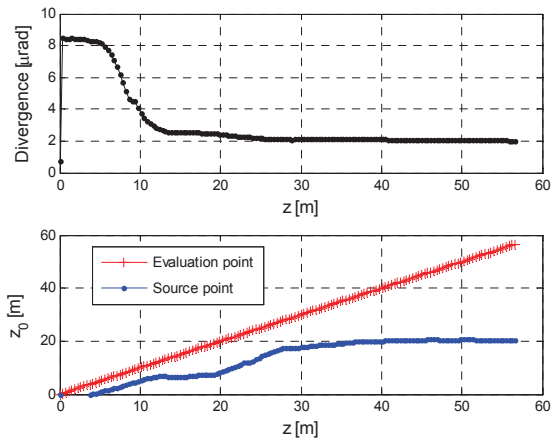

Figure 6: Radiation divergence (top) and effective source position (bottom, blue) along the undulator for the LP mode at a radiation wavelength of 1 Å. The red curve of the bottom plot indicates the point where the evaluation is done ($z_0 = z$).

WAKEFIELD EFFECTS

Longitudinal wakes in the undulator can modify the energy of the electrons and therefore degrade the FEL performance by shifting the resonance condition. We have studied the wake effects due to resistive wall and surface roughness for the LP mode and a radiation wavelength of 1 Å. For the calculation of the wakes we follow the procedure of Refs. [7, 8] and we assume the parameters indicated in Table 2.

Table 2: Parameters for the Wakefield Calculations

Material	Copper
Separation of parallel plates	4.4 mm
Corrugation amplitude	100 nm
Corrugation period	10 μm

Figure 7 shows the wake along the bunch ($\zeta = 0$ indicates the head of the bunch). The current profile as well as the contributions of the resistive wall and the surface roughness are indicated. Although the current profile is slightly different than the one showed in Figure 1, the results are expected to be equivalent. We note that the final wake does not depend significantly on the current spike in the head of the bunch and on the visible ripples in the current profile. The ripples are due to the low number of particles used in the start-to-end simulations in that case, which yield a larger shot-noise level for the longitudinal space-charge calculations in the elegant tracking.

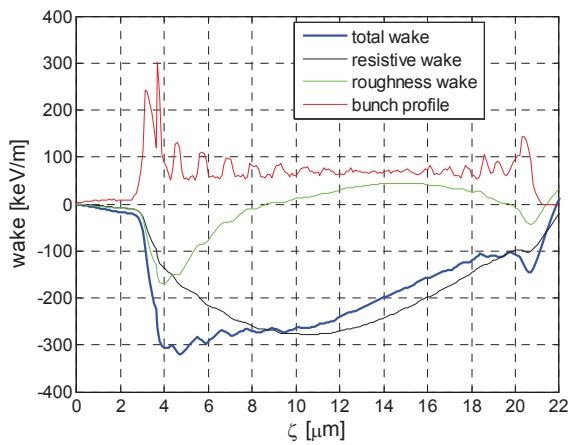

Figure 7: Undulator wakes along the bunch for the LP mode (the beam charge is 200 pC).

The effect of the wakes can be compensated by tapering the undulator. Figure 8 shows the relative macropulse FEL energy at the end of the undulator for different linear pre-saturation taper amplitudes, with and without considering the wakes. In this case we did not optimize the post-saturation tapering. Without tapering, the FEL energy decreases by a factor of 2 due to the wakes. The optimum tapering without considering the wakes is about 0.05 %. In the presence of wakes, the taper amplitude has to be further increased to about 0.096 % to compensate for the additional energy loss due to wakes. The final FEL performance is not significantly degraded due to wakes: the optimum FEL performance for the 2 cases differ only for about 5%.

ISBN 978-3-95450-133-5

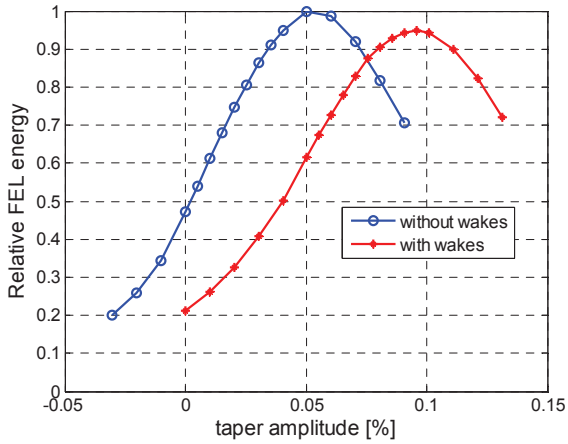

Figure 8: FEL relative pulse energy vs taper gradients. Tapering reduces the wakefield effects to a ~5 % level.

CONCLUSIONS AND OUTLOOK

We have presented the expected SASE performance for the hard X-ray beamline of SwissFEL based on electron distributions obtained from start-to-end simulations. The FEL macropulse energy is significantly higher than the one obtained with the design parameters and presented in Ref. [1] – for example for the LP mode, we expect to obtain about 1.5 mJ of FEL energy, a factor of ~10 higher than with the design parameters. The improvement can be explained by three factors: smaller normalized emittances, a better β-function along the undulator optimized for such emittances, and undulator tapering. Based on our slice and thermal emittance measurements at the SwissFEL Injector Test Facility [9, 10] we presently expect to obtain significantly smaller emittances than the design ones – for instance, for the LP mode the design emittance is 0.43 μm and the currently expected is about 0.20 μm.

For the LP mode, the spike at the head of the bunch (see Figure 1) contributes to the FEL performance. In the start-to-end simulations we have considered 1D CSR effects in the bunch compressors and longitudinal space-charge along the linac. We will perform more advanced calculations to benchmark our 1D simulation results.

Apart from the two standard operation modes, SwissFEL will have two additional special configurations: a large-bandwidth mode with 200 pC charge in which the FEL bandwidth will reach the few-percent level, and a ultra-short pulse mode that will generate attosecond pulses with three compression stages. Detailed start-to-end simulations for these modes will be presented in a future opportunity.

ACKNOWLEDGMENTS

We thank Simona Bettoni and Bolko Beutner for the work to generate the particle distributions that we used as input for the FEL simulations.

REFERENCES

[1] R. Ganter et al, PSI Report No. 10-04, 2012.
[2] G. Geloni et al, DESY report 10-053, 2010.
[3] K. Floettmann, *ASTRA - A Space Charge Tracking Algorithm*. DESY, Hamburg, Germany.
[4] M. Borland, Advanced Photon Source Report No. LS-287, 2000.
[5] S. Reiche, NIM A **429**, 243, 1999.
[6] S. Reiche. Proceedings of the FEL'06, Berlin, Germany, 126-129 (2006).
[7] K. L. F. Bane and G. Stupakov SLAC Report N0. SLAC-PUB-10707, 2004.
[8] G. Stupakov and S. Reiche. Proceedings of the FEL'13, New York, USA, 127-131 (2013).
[9] E. Prat et al. Proceedings of the FEL'13, New York, USA, 200-204 (2013).
[10] E. Prat et al. Proceedings of this conference.

ISBN 978-3-95450-133-5